J. Membrane Biol. 150, 231–241 (1996)

The Journal of
Membrane
Biology

Reaction Kinetics of the Vacuolar H^+-Pumping ATPase in *Beta vulgaris*

J.M. Davies[1], **D. Sanders**[1], **D. Gradmann**[2]
[1]Plant Laboratory, Department of Biology, University of York, P.O. Box 373, York YO1 5YW, United Kingdom
[2]Pflanzenphysiologisches Institut der Universität, Untere Karspüle 2, 37073 Göttingen, Germany

Received: 19 July 1995/Revised: 18 December 1995

Abstract. Vacuolar-type H^+-ATPases (V-ATPases) are ubiquitous in eukaryote endomembranes, where they are responsible for lumenal acidification. The ratios of H^+ translocated per ATP hydrolyzed (which may be important in controlling the activity of these pumps) have previously been found to be variable, noninteger and sensitive to cytosolic as well as lumenal pH. The mechanistic implications of these findings are explored here with reaction kinetics. Experimental data for this analysis comprise supra- and superlinear V-ATPase current-voltage relationships, isolated as bafilomycin-sensitive currents in vacuolar membranes from *Beta* using the ''whole vacuole'' patch clamp configuration. Whereas simple models with one reaction cycle fail to provide an adequate description of the data (mainly because of a weak sensitivity of the zero-current voltage to the transmembrane pH gradient), a model with two linked reaction loops allowing partial coupling of H^+ translocation to ATP hydrolysis does provide good descriptions. All experimental data obtained with the same vacuolar pH (4.3) could be reduced to a model with eleven independent parameters. Best fits have been obtained on the basis of a binding domain possessing 3 H^+ binding sites per ATP hydrolyzed and a net charge of −2 when unoccupied. The enzyme could reorientate its access site between the vacuolar and cytoplasmic side when zero, one or three H^+ are bound.

Key words: *Beta* — Coupling ratio — Partial coupling — V-ATPase

Introduction

Active transport of H^+ in endomembranes of eukaryotic cells is facilitated by V-type ATPases (Harvey, 1992), which are related to the ubiquitous F-type ATPases in the energy-conserving membranes of prokaryotes, mitochondria and chloroplasts. Ion-motive ATPases interconvert metabolic energy and electrochemical ion gradients. Although the structure and biochemistry of V-type ATPases have become increasingly well understood (Sze et al., 1992), their electrochemical function has yet to be described in quantitative physicochemical terms. The V-type ATPases of vascular plant vacuolar membranes afford an opportunity to examine this subject on the experimental basis of steady-state current-voltage ($I(V)$) relationships of this enzyme. These relationships are essentially equivalent to enzyme kinetics, where the membrane current represents the turnover of charge (H^+) translocation and voltage corresponds to the (logarithm of the) substrate concentration. Since $I(V)$ relationships of the vacuole can be determined by patch clamp techniques and since bafilomycin is available as a potent, noncompetitive inhibitor of V-type ATPases (Bowman, Siebers & Altendorf, 1988; White, 1994), the specific $I(V)$ relationship of the vacuolar H^+-ATPase can be isolated from whole membrane $I(V)$ relationships as a bafilomycin-sensitive current (Davies, Hunt & Sanders, 1994).

The operational transport coupling ratio, c, of H^+ translocated per ATP hydrolyzed has been estimated for the V-ATPase in *Beta* vacuoles from bafilomycin-sensitive $I(V)$ relationships (Davies et al., 1994). The method involved comparison of the zero-current voltage (V_r) of the pump $I(V)$ relationship with the free energy of ATP hydrolysis for defined cytoplasmic and vacuolar pH values (pH_{cyt} and pH_{vac} respectively). The resultant value of c was found to decrease with increasing pH_{cyt} at set pH_{vac} but increased with increasing pH_{vac} at set pH_{cyt}. The estimates of c lay in the range 1.75 to 3.28. These estimates of c were based on the assumption of tight coupling between H^+ translocation and ATP hydrolysis in a single reaction loop.

Correspondence to: J. Davies

However, the operational H^+:ATP coupling ratio, *c*, should be distinguished from the H^+:ATP stoichiometry, *n*, which is defined as the maximum number of H^+ translocated per reaction cycle when all binding sites are occupied (Läuger, 1991). One possible explanation, both for the noninteger estimates of *c* and for the dependence of *c* on pH is that coupling of H^+ translocation and ATP hydrolysis is not tight; i.e., that depending on pH, a reaction cycle can take place with not all of the *n* H^+ binding sites occupied. The corresponding reaction scheme for this more general approach requires more than one reaction cycle, each with a discrete (and integer) value of *n*.

In the present study, the proposed variable coupling ratio of the V-ATPase has been examined in greater detail by extending the data of Davies et al. (1994) to include a range of pH_{cyt} values at fixed pH_{vac}. Moreover, the problem has been studied in more detail by using the entire kinetic information comprised by the nonlinear *I*(*V*) relationships of the V-ATPase. The case of a single V-ATPase isoform is considered, which may have $n \geqslant 3$, but for which ATP hydrolysis can take place without translocation of the full H^+ complement. Whereas the stoichiometry of the V-ATPase is as yet unknown, the apparent coupling ratios may be approached on the basis that H^+ translocation and ATP hydrolysis can, depending on conditions, be partially coupled. The corresponding reaction system of this more general approach requires more than one reaction cycle. A reaction system with more than one closed loop has been used for the physicochemical description of the results in straightforward terms of mass action effects of H^+ as the transported substrate of the enzyme.

Materials and Methods

Experimental

Vacuole Preparation and Solutions

Red beet plants (*Beta vulgaris*) were grown and storage tissue vacuoles isolated as described by Davies, Rae & Sanders (1991). Fresh vacuoles were prepared for each experiment. Solutions were designed to put V_r of the V-ATPase into measurable range. The basal bathing and pipette media (corresponding to cytoplasmic and vacuolar solutions respectively) contained (in m*M*): 100 choline-Cl, 5 $MgCl_2$, 0.1 EGTA and 20 Tris. pH was adjusted with 3,3-dimethylglutarate. *D*-sorbitol (98% purity, Sigma Chemical) was added to bathing and pipette solutions to raise their osmolarities to 100–150 mosM above that of an expressed cell sap sample. Adenosine nucleotides were added to the bathing medium as Tris salts, P_i as the free acid. An excess concentration (600 nM) of the specific and tightly-binding V-ATPase inhibitor bafilomycin A_1 (a gift from Smith Kline Beecham and referred to here as lots I and II) was added in a dimethyl sulphoxide (DMSO) solution to that containing ATP/ADP/P_i. DMSO (previously found to have no apparent effect on the control membrane *I*(*V*) characteristic; Davies et al., 1994) was added to all other solutions to the same final concentration (which did not exceed 0.1% v/v).

Recording of Current-voltage Relationships

The specific patch clamp protocol was as described by Davies et al. (1991, 1992). Whole vacuole *I*(*V*) recordings were performed during continuous perfusion of the bathing medium at 20 ± 1°C. A bipolar staircase voltage clamp protocol was applied from a 0 mV baseline holding voltage (PClamp Software, Axon Instruments, Foster City, CA); pulses were of 9-sec duration to allow current to achieve a steady state and were delivered in 10 mV increments up to ±90 mV. The *I*(*V*) characteristics of the membrane were first determined under control conditions, then in the presence of ATP/ADP/P_i and finally in the additional presence of bafilomycin. Vacuoles were exposed to bafilomycin until the measured *I*(*V*) characteristic remained stable. For the bafilomycin lot II (used in experimental sets A, B and H; pH_{cyt}/pH_{vac} 7.5/4.3, 7.0/4.3 and 7.0/5.3 respectively) vacuoles were typically exposed to the inhibitor for 12 min; for the lot I (used in the remaining experimental sets) exposure was for 4 min. Bafilomycin, in the absence of V-ATPase substrates and products, had no discernable effect on the control membrane *I*(*V*) relationship when sampled after 12-min exposure.

Derivation of the Bafilomycin-sensitive Current

Current was filtered at 3 kHz and sampled from the last 1 sec of the voltage pulse. Liquid junction potentials were corrected as described by Hanrahan, Alles & Lewis (1985). The *I*(*V*) relationship of the V-ATPase was obtained by subtraction of the *I*(*V*) relationship of the energized membrane in the presence of bafilomycin from that determined solely in the absence of that inhibitor (Davies et al., 1994). This difference *I*(*V*) relationship yielded bafilomycin-sensitive currents and V_r was the interpolated zero-current intercept. Apparent values of *c* (taken to equal *n* on the assumption of complete coupling) were then obtained by substituting the measured V_r into Eq. (1):

$$V_r = (RT/nF) \cdot \ln\{([P_i][ADP][H^+]^n{}_{vac})/(K_{ATP}[ATP][H^+]^n{}_{cyt})\} \quad (1)$$

where subscripts cyt and vac denote cytosolic and vacuolar compartment respectively, K_{ATP} is the apparent equilibrium constant for ATP hydrolysis and *R, T, F* have their usual meanings. For polarity convention, membrane voltage (*V*) was defined with reference to the lumenal compartment (i.e., $\psi_{cyt} - \psi_{vac}$). Thus, positive (outward) current was taken to be the exit of positive charge from the cytoplasm into the vacuolar lumen.

Estimation of Apparent Equilibrium Constants for ATP Hydrolysis (K_{ATP}) and ΔG_{ATP}

Values of K_{ATP} in Eq. 1 were calculated by as given by Davies et al. (1993, 1994). Briefly, the equilibrium constant for the reference reaction (K_{ref}) was 9.8×10^5 M. Apparent values for K_{ATP} were determined for each set of ionic conditions by substitution into Eq. 2:

$$K_{ATP} = K_{ref} \cdot ([HATP^{3-}]/[ATP])/([H_2PO_4^-]/[P_i]) \cdot ([HADP^{2-}]/[ADP]) \quad (2)$$

The resultant K_{ATP} values for ligand concentrations of 5/5/10 mM ATP/ADP/P_i respectively were (in M): pH_{cyt} 7.0, 5.20×10^5; pH_{cyt} 7.5, 1.06×10^6; pH_{cyt} 7.6, 1.31×10^6; pH_{cyt} 8.0, 2.9×10^6; and for ligand concentrations of 1/5/10 mM at pH_{cyt} 8.0, 1.27×10^6 M. The free

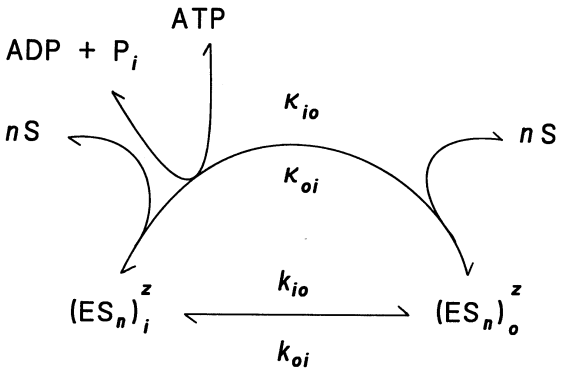

Fig. 1. Reaction scheme of a 2-state model (according to Hansen et al., 1981) for the description of $I(V)$ relationships of an ATP-driven pump for n molecules of the substrate S, with a charge z per ATP hydrolyzed.

energy of ATP hydrolysis (ΔG_{ATP}) was calculated as described by Davies et al. (1993).

Theoretical Approaches to Reaction Kinetic Modeling

Two-state Model

The simple reaction kinetic scheme shown in Fig. 1 has been introduced by Hansen et al. (1981) for the description of steady-state current-voltage relationships of electrogenic pumps with one voltage-sensitive reaction step. This reversible charge translocation reaction between inside (i) and outside (o) is described by the voltage-sensitive rate constants k_{io} and k_{oi}, whereas the voltage-insensitive steps in the reaction cycle are summarised by two, voltage-insensitive, global rate constants κ_{io} and κ_{oi}. Voltage-sensitivity is introduced as

$$k_{io} = k^0_{io}\exp(au/2), \tag{3a}$$

and

$$k_{oi} = k^0_{oi}\exp(-au/2) \tag{3b}$$

where the superscript ^{0} denotes the rate constants k at zero voltage; u ($=V_mF/(RT)$) is the reduced membrane voltage and the coefficient α expresses the degree of voltage-sensitivity. This coefficient comprises the number and polarity of charges, z, which are translocated during each reaction cycle. It may also comprise an empirical factor f ($0 < f < 1$), so we may write $\alpha = fz$. In the most simple case α is unity. A symmetrical Eyring barrier (Läuger & Stark, 1970) appears in Eq. 3 by setting the denominator of the exponents to 2.

The voltage-sensitive parameters k_{io} and k_{oi} of the 2-state model may actually subsume voltage-insensitive reactions of the true Class I higher-state reaction cycle, such as substrate binding (for details *see* Hansen et al., 1981 and Gradmann, Klieber & Hansen, 1987). However, for simplicity, substrate binding has been assigned here only to the voltage-insensitive, global rate constants κ_{io} and κ_{oi} of the 2-state model. Thus, when the H^+ concentrations, $[H^+]$, are considered, the voltage-independent rate constants κ_{io} and κ_{oi} should be

$$\kappa_{io} = \kappa^0_{io}[H^+]^n_o, \tag{4a}$$

and

$$\kappa_{oi} = \kappa^0_{oi}[H^+]^n_i, \tag{4b}$$

where the superscript ^{0} denotes κat 1 M substrate concentration and n is the stoichiometry. With the definitions above, the $I(V)$ relationship given by the model in Fig. 1 becomes

$$I(V) = zFN(k_{io}\kappa_{oi} - k_{oi}\kappa_{io})/(k_{io} + k_{oi} + \kappa_{io} + \kappa_{oi}), \tag{5}$$

where N is the total density of transporter molecules (in mol · m^{-2}), i.e., the sum of N_i and N_o in Fig. 1 ($(ES_n)_i$ and $(ES_n)_o$ respectively; Hansen et al., 1981). If the true, higher state reaction system comprises one cycle, microscopic reversibility requires that

$$k^0_{io}\kappa^0_{oi}/(k^0_{oi}\kappa^0_{io}) = \exp(\Delta G_{ATP})/(nRT) \tag{6}$$

and the zero-current voltage

$$V_r = RT/F\{-\Delta G_{ATP}/(nRT) + \ln([S]_o/[S]_i)\} \tag{7a}$$

or

$$V_r = -\Delta G_{ATP}/nF + (59\text{ mV})\Delta\text{pH}. \tag{7b}$$

However, in cases where the real reaction system comprises more than one closed loop and/or more than one voltage-sensitive reaction step, microscopic reversibility implied within the pseudo two-state description of the real higher order model no longer holds. Nevertheless, the two-state formalism has been retained to enable fits to experimental data using Eq. 5. Correspondingly, the resulting sets of four apparent rate constants are not meaningful in strictly thermodynamic terms. They can be used, however, for qualitative considerations of the energetics of the entire system on the basis of the left-hand-side of Eq. 6. Similarly, the different values of α used as part of this fitting can then be used to assess the charge relations of the complete reaction system for further model expansion.

Six-state Model Incorporating Incomplete Coupling

Although the existence of 3 or more H^+ binding sites could be represented by a variety of reaction schemes, higher order modeling of the transport system has been restricted to one 6-state model describing two explicit reaction loops for ATP hydrolysis and H^+ translocation, which are linked by one common reaction step. This selection allows a determination of the capacity of such models to describe the observations in relatively simple terms. The reaction kinetic scheme shown in Fig. 2 has been used to describe the V-ATPase currents as functions of the cytoplasmic H^+ concentration, $[H^+]_{cyt}$, vacuolar H^+ concentration, $[H^+]_{vac}$, and the estimated free energy of ATP hydrolysis, ΔG_{ATP}. Reaction schemes such as this, which incorporate more than one voltage-sensitive trans-membrane pathway are termed Class N models (here, N = II or III) to distinguish them from models in which a single transmembrane pathway is present (Class I models: Hansen et al., 1981).

The reaction scheme comprises six states (which are numbered arbitrarily from 1 to 6) and fourteen rate constants (k_{ij}) which describe the transition from state i to state j respectively. Translocation of a single H^+ through the membrane is afforded by the $4 \rightleftharpoons 3$ transition (with forward and backward rate constants k_{43} and k_{34} respectively). An additional two H^+ are translocated by the $1 \rightleftharpoons 2$ transition (k_{12}, k_{21}). Thus the first closed loop of the reaction scheme ($5 \rightleftharpoons 4 \rightleftharpoons 3 \rightleftharpoons 6 \rightleftharpoons 5$) allows a partially-coupled reaction; i.e., translocation of H^+ without binding/translocation of the complement of three H^+. To ensure microscopic reversibility, the number of independent rate constants in the reaction system with two closed loops is reduced by two for the conditions

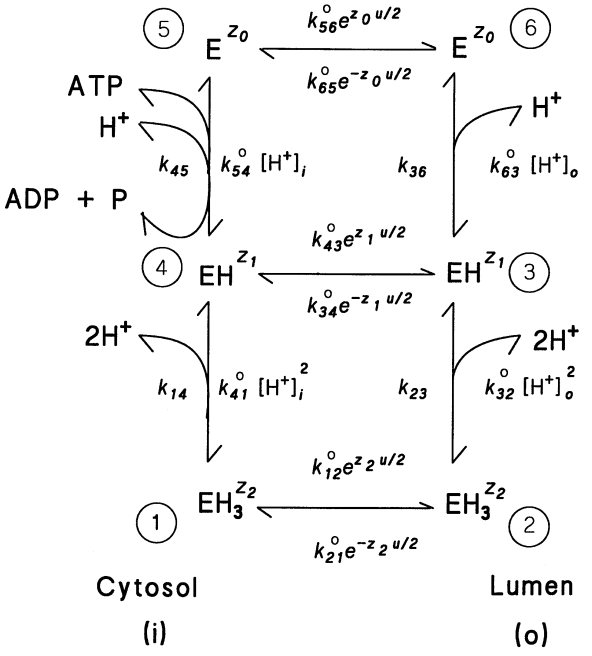

Fig. 2. Reaction scheme of the 6-state model incorporating variable coupling; detailed description in Materials and Methods.

$$k^0_{12}k_{23}k^0_{34}k^0_{41}/(k^0_{21}k^0_{32}k^0_{43}k_{14}) = 1 \tag{8a}$$

and

$$k^0_{54}k^0_{43}k_{36}k^0_{65}/(k_{45}k^0_{34}k^0_{63}k^0_{56}) = \exp(\Delta G_{ATP}/(RT) \tag{8b}$$

at 1 M $[H^+]_{cyt}$ and $[H^+]_{vac}$, and at zero transmembrane voltage, V_m. If follows that if the relationships of Eq. 8*b* were to reflect the situation correctly, ''energization'' should not be assigned necessarily to an individual reaction step (such as k_{54}) but can be distributed across all reactions in a closed reaction loop.

The stoichiometry of the fully coupled cycle (i.e., $k_{34},k_{43} = 0$) is nH$^+$/ATP. For partially coupled conditions ($k_{34},k_{43} > 0$) two H^+ binding steps, with integer values for H^+ of n_1 and n_2, are considered with $n_1 + n_2 = n$. As the binding domain of the unoccupied states 5 and 6 has the charge number z_0 and the charge number of H^+ is unity ($z = 1$), then the charge of the partially occupied states 4 and 3 becomes $z_1 = z_0 + zn_1$ and that for the fully occupied states (1 and 2) $z_2 = z_1 + zn_2$.

Equation 8 allows for the input of energy from ATP hydrolysis. V_m enters the system through the membrane translocation steps

$$k_{56} = k^0_{56}\exp(z_0u/2), \tag{9a}$$

$$k_{65} = k^0_{65}\exp(-z_0u/2), \tag{9b}$$

$$k_{43} = k^0_{43}\exp(z_1u/2), \tag{9c}$$

$$k_{34} = k^0_{34}\exp(-z_1u/2), \tag{9d}$$

$$k_{12} = k^0_{12}\exp(z_2u/2), \tag{9e}$$

$$k_{21} = k^0_{21}\exp(-z_2u/2), \tag{9f}$$

with symbols equivalent to those in Eqs. 3*a*,*b*.

The effects of cytoplasmic and vacuolar $[H^+]$ are accounted for by the apparent rate constants for H^+ binding thus:

$$k_{54} = k^0_{54}[H^+]^{n1}_{cyt}, \tag{10a}$$

$$k_{41} = k^0_{41}[H^+]^{n2}_{cyt}, \tag{10b}$$

$$k_{63} = k^0_{63}[H^+]^{n1}_{vac}, \tag{10c}$$

$$k_{32} = k^0_{32}[H^+]^{n2}_{vac}, \tag{10d}$$

where the superscript ^{0} here denotes the fundamental rate constants at 1 M substrate concentration.

If all rate constants are known, the steady-state probabilities, p_i, of the six states can be calculated (Klieber & Gradmann, 1993) and the membrane current I (in A.m^{-2}) through the entire system (with a constant density, N, of pumps in the membrane as defined previously) is then given by

$$I = FN\{z_0(p_5k_{56} - p_6k_{65}) + z_1(p_4k_{43} - p_3k_{34}) + z_2(p_1k_{12} - p_2k_{21})\}. \tag{11}$$

Fitting Strategies

Intervacuolar variation in absolute magnitude of current generated by the V-ATPase precluded a reliable estimate of N and hence the determination of absolute rate constants. Therefore, after appropriate scaling of the data (*see below*), the model rate constants have been normalized to $k^0_{io} = 1$ sec^{-1} in the 2-state model (Fig. 1) and $k^0_{12} = 1$ sec^{-1} in the 6-state model (Fig. 2). This reduced the number of independent parameters by one in each model. As stated previously, to ensure microscopic reversibility (Eq. 8), the number of independent parameters of the 6-state model was reduced by another two; thus eleven free model parameters remained to be fitted. For both models, individual parameters were fitted using an iterative least squares routine. Increments were initially set at ±5%, were decreased when the error of the fit stabilized and were typically reduced to below 0.05%.

The 2-state model was applied to individual $I(V)$ relationships (from all experimental conditions), with α either fixed ($z = 1$, 2, or 3) or fitted also. The 6-state model was applied to mean $I(V)$ relationships for each experimental condition. For the 6-state model, the resultant fits were heavily dependent on the starting values of the fit parameters. To decrease the likelihood of erroneous solutions as the fit procedure becomes entrapped in local minima (a common problem for multiparameter fits), the main fitting routine was repeated with various sets of start parameters. The first set was chosen arbitrarily with the aim of placing model currents and reversal voltages in the order of magnitude of the measured data. New sets of start parameters were chosen by sequential increasing and decreasing scalings of the eleven free model parameters by a factor of 100. Cycling of this routine was automatic and the best fit after 20 cycles was accepted as a solution. These solutions cannot be considered unique but as reasonable quantitative approaches which serve to indicate whether the general fully and partially coupled models under consideration are competent to describe the data.

Results

Application of a 2-State Model

Steady-state current-voltage $I(V)$ relationships of the vacuolar H^+-ATPase have been determined by subtrac-

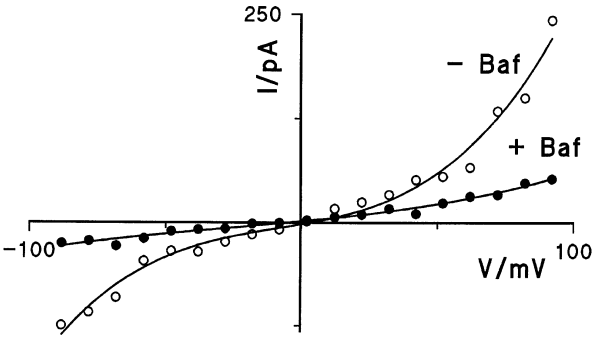

Fig. 3. Example of whole membrane *I*(*V*) relationships obtained from a single vacuole before and after exposure to 600 nM bafilomycin A_1; ligand concentrations were (in mM): 5 ATP, 5 ADP, 10 P_i, with pH_{cyt} 7.5, pH_{vac} 4.3.

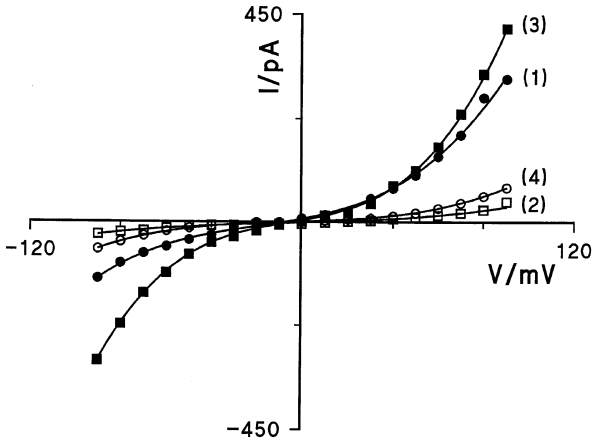

Fig. 4. Bafilomycin-sensitive V-ATPase *I*(*V*) relationships obtained from 4 separate vacuoles (in mM): 5 ATP, 5 ADP, 10 P_i; pH_{cyt} 7.0, pH_{vac} 4.3) and subjected to a simultaneous fit of the 2-state model (Eq. 3). The absolute rate parameters were k^0_{io} = 17.2 sec^{-1}, k^0_{oi} = 17.0 sec^{-1}, κ_{io} = 401.7 sec^{-1} and κ_{oi} = 678.5 sec^{-1}; κ = 2. Scaling factors for individual *I*(*V*) relationships: (1) 1.0; (2) 0.17; (3) 1.44; (4) 0.26.

tion of the bafilomycin-sensitive current from the overall *I*(*V*) relationship of the energized membrane. An example of whole membrane *I*(*V*) relationships prior to and following bafilomycin treatment is shown in Fig. 3. Equation 1 was used to derive an initial estimate of *c* for each *I*(*V*) difference relationship. The mean value of *c* for each experimental condition varied with pH_{cyt} and pH_{vac} as described previously (Davies et al., 1994). For example, with pH_{vac} set at 4.3, *c* decreased from 2.95 at pH_{cyt} 7.0 to 2.14 at pH_{cyt} 8.0 and when pH_{cyt} was set at 7.0 but pH_{vac} raised from 4.3 to 5.3, *c* was estimated to be 4.46. Errors on the estimate of *c* amount to no more than 0.15.

Scaling Factors

Figure 4 shows the ATPase *I*(*V*) relationships from four vacuoles under the same experimental conditions (pH_{cyt} 7.0, pH_{vac} 4.3). It demonstrates a similarity in the shape of the relationships but considerable variation in the magnitude of the absolute currents obtained. Therefore, individual *I*(*V*) relationships have been standardized by setting k^0_{io} to 1 sec^{-1}, as described in Materials and Methods (Fitting Strategies).

Determination of Voltage-Sensitivity

All individual ATPase *I*(*V*) relationships obtained under each experimental condition have been subjected to fits using Eq. 5, with α either constrained (α = 1, 2, or 3) or unconstrained. A comparison of four fits of the model for an individual *I*(*V*) relationship obtained at pH_{cyt} 7.0, pH_{vac} 4.3 (taken from Fig. 4) is shown in Fig. 5. In this case equally good fits were obtained with α = 2 or 3, with the unconstrained fit yielding α = 2.01. The overall results (compiled in Table 1) show that for the entire system, α = 2 is most appropriate. The fitted values of α scatter around 2 (1.98 ± 0.03). Examples of fits using α = 2 for individual *I*(*V*) relationships from each experimental set are given in Fig. 6.

As shown in Fig. 6, the *I*(*V*) relationships recorded in this study exhibited both sigmoidal (e.g., Fig. 6*F* and *H*) and ''*N*-shaped'' characteristics (i.e., a shallow slope in the central voltage region and steep branches to either side: Fig. 6*A–E* and *G; see also* Rakowski et al., 1991, for an example with the (Na^+/K^+-ATPase). The shapes of the *I*(*V*) relationships are determined by the (relative) parameter values (k^0_{io}, k^0_{oi}, κ_{oi} and κ_{io}) of the model (Hansen et al., 1981). Thus the 2-state reaction kinetic model (Fig. 1) can fit both ''*N*''-shaped and sigmoidal *I*(*V*) characteristics. Furthermore, the V-ATPase *I*(*V*) relationships recorded here are described reasonably well by Eq. 5 (Table 1, Fig. 6).

For the determination of the four system parameters (k^0_{io}, k^0_{io}, κ_{oi} and κ_{io}) from observable parameters, Hansen et al. (1981) focused upon four specific observables; i.e., the two saturation currents for large positive and negative voltage displacements from the zero-current voltage (V_r), on V_r itself and on the short circuit current, I_{sc}. In general however, any set of four independent observable parameters may serve this purpose. Although most of the *I*(*V*) relationships presented here did not exhibit saturation currents, they were sufficiently well-defined by the given sets of data points to ensure that the fitting routine (using Eq. 5) converged at similar solutions for different sets of start parameters.

As judged by immediate visual impression, fits such as those displayed in Fig. 6 suggested the 2-state model shown in Fig. 1 to be appropriate. The numerical results,

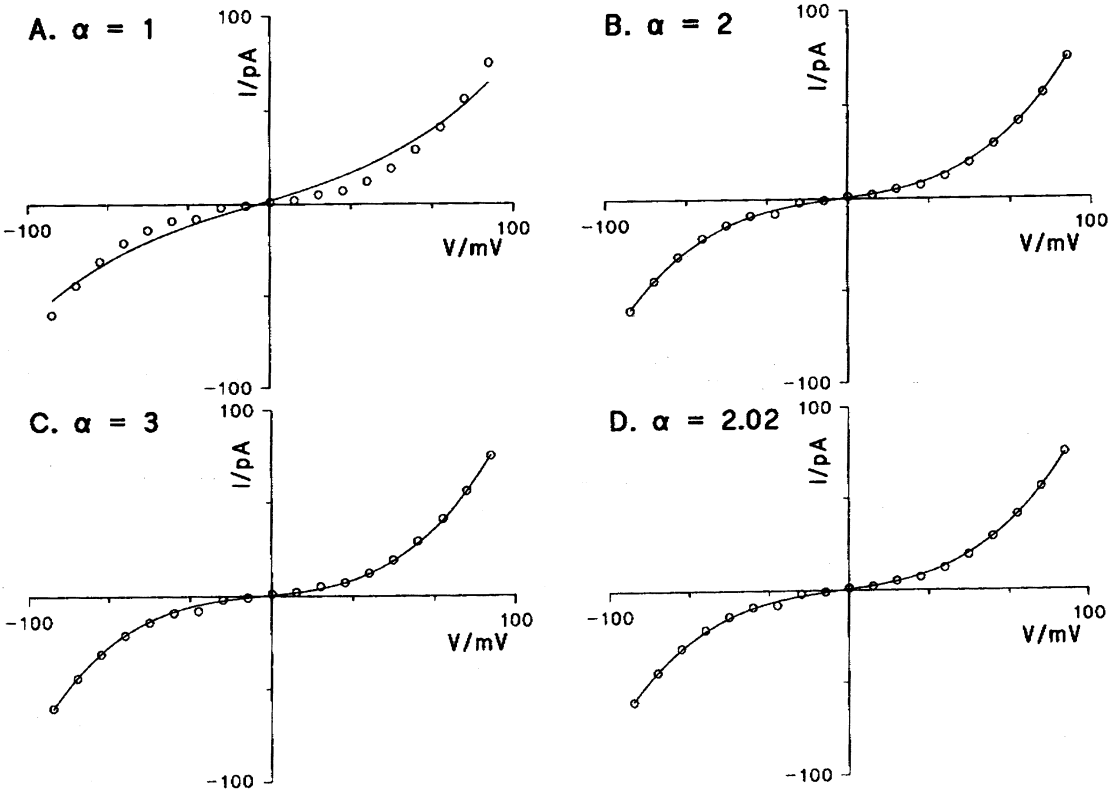

Fig. 5. Application of the 2-state model (Eq. 3) to a V-ATPase $I(V)$ relationship obtained with (in mM): 5 ATP, 5 ADP, 10 P_i and pH_{cyt} 7.0, pH_{vac} 4.3. The value of α was constrained at 1 (*A*), 2 (*B*), 3 (*C*) or unconstrained (*D*).

however, render them incompatible with the principle of microscopic reversibility. Taking the parameter ratio

$$Q = (k^0_{io}\kappa_{oi})/(k^0_{oi}\kappa_{io}) = [H^+]_{cyt}/[H^+]_{vac}\exp(\Delta G_{ATP}/(nRT)), \quad (12)$$

an *increase* of the pH gradient ($\Delta pH = pH_{cyt} - pH_{vac}$) of one unit should result in a corresponding *decrease* of Q by factor ten (ignoring pH_{cyt}-dependent changes in ΔG_{ATP}). In practice, the fitted sets of system parameters did not support such a relationship; for example, sets *B* and *D* (Table 1).

Table 1. Summary of goodness of fits, using the 2-state model, applied to all experimental data sets (trials per set in parentheses).

Set	*A* (2)	*B* (4)	*C* (2)	*D* (2)	*E* (3)	*F* (2)	*G* (2)	*H* (2)
pH_{cyt}/pH_{vac}	7.5/4.3	7.0/4.3	8.0/4.3	8.0/4.3	7.6/3.9	7.0/4.8	7.6/4.8	7.0/5.3
Error relative to α = 2								
α = 1	4.53	4.42	2.89	1.19	0.75	2.60	3.84	1.07
α = 2	1.0	1.0	1.0	1.0	1.0	1.0	1.0	1.0
α = 3	1.83	1.39	0.99	1.26	0.77	1.88	1.60	1.08
Fitted α	2.01	1.99	2.05	2.04	2.09	1.82	1.99	1.91
Q value for α = 2, per trial								
	(1) 1.38	(1) 2.43	(1) 1.19	(1) 6.29	(1) 13.75	(1) 2.18	(1) 0.97	(1) 1.24
	(2) 1.18	(2) 0.56	(2) 1.51	(2) 1.42	(2) 1.32	(2) 1.05	(2) 1.23	(2) 1.29
		(3) 1.51			(3) 0.02			
		(4) 1.33						

Results are shown for α fixed at 1, 2, 3 or fitted and the mean error of the fit expressed relative to that found for α = 2. The parameter ratio Q (given by Eq. 12) was calculated with α set at 2 for each experimental trial in all data sets. The ligand concentrations used were (in mM: 5 ATP, 5 ADP, 10 P_i except for set *C* where ATP was 1 mM.

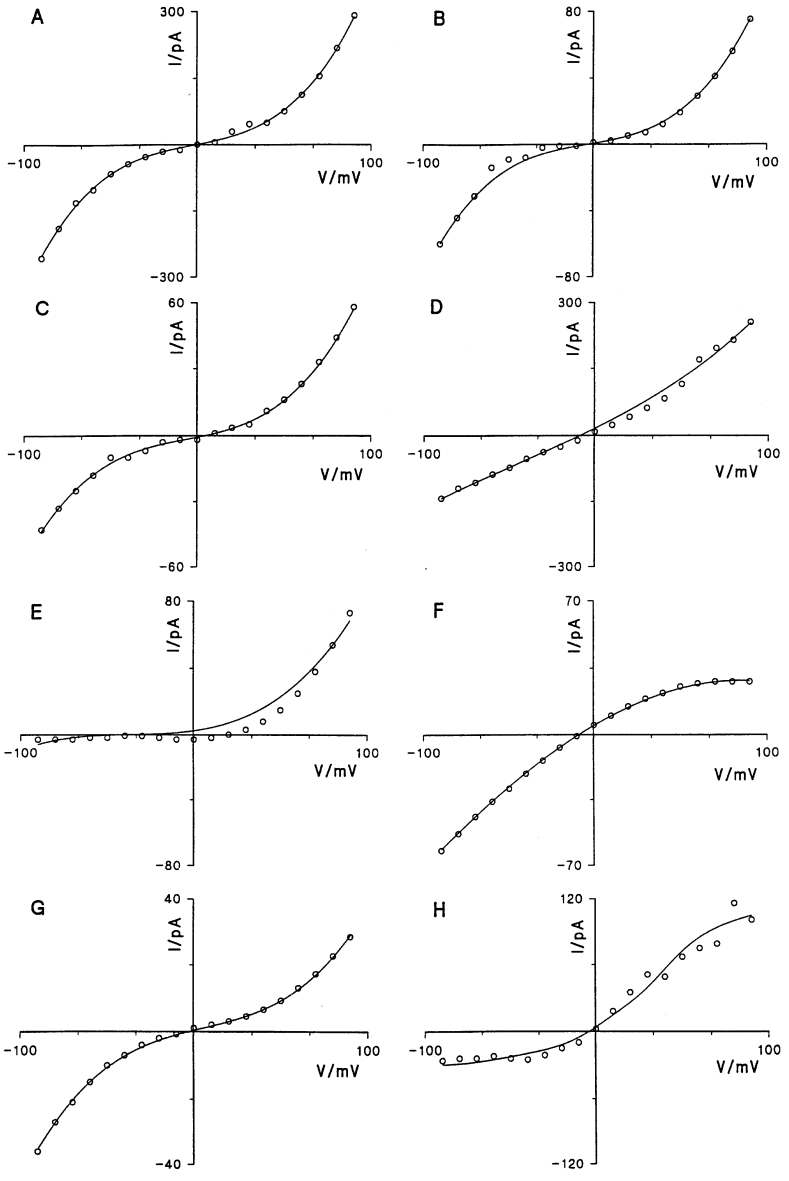

Fig. 6. Representative examples of 2-state model fits by Eq. 3 to individual $I(V)$ relationships from each set of experimental conditions; $\alpha = 2$, ligand concentrations (in mM): 5 ATP, 5 ADP, 10 P_i except for set *C* (1 mM ATP). Fitted rate constants not listed individually but subsumed in Q values presented in Table 1.

Application of a Six-State Model

Figure 7 shows the result of attempting a simultaneous fit of the 6-state model (Fig. 2) to the measured $I(V)$ relationships from experimental sets *A*, *B*, *C* and *D*. Vacuolar pH was constant at pH 4.3 but pH_{cyt} varied from 7.0 (set *B*), 7.5 (set *A*) to 8.0 (sets *C*, *D*) and ATP varied from 1 mM (set *C*) to 5 mM (sets *A*, *B*, *D*). The fitting strategy allowed variations in the values of n_1 and n_2 of the individual reaction steps. This encompassing fit yielded satisfactory descriptions of these data. Some of the variations in n_1 and n_2 have been tested, as indicated in Table 2. With $n = 2$ ($n_1 = 1$, $n_2 = 1$), the model replicated individual $I(V)$ relationships quite well (*data not shown*), but failed to describe several $I(V)$ relationships simultaneously. Fits with $n = 3$ ($n_1 = 1$, $n_2 = 2$) showed some improvement; from such fits, those with a binding domain charge (z_0) of −2 (as shown in Fig. 2) were better than those with $z_0 = 0$ (the curvature was too great as $z_2 = 3$) and $z_0 = -1$. With the fundamental demonstration that the model was capable of the description of various $I(V)$ relationships under different substrate conditions and constant pH_{vac}, the search for fits with further versions of the model (e.g., $n_1 = 2$, $n_2 = 1$)

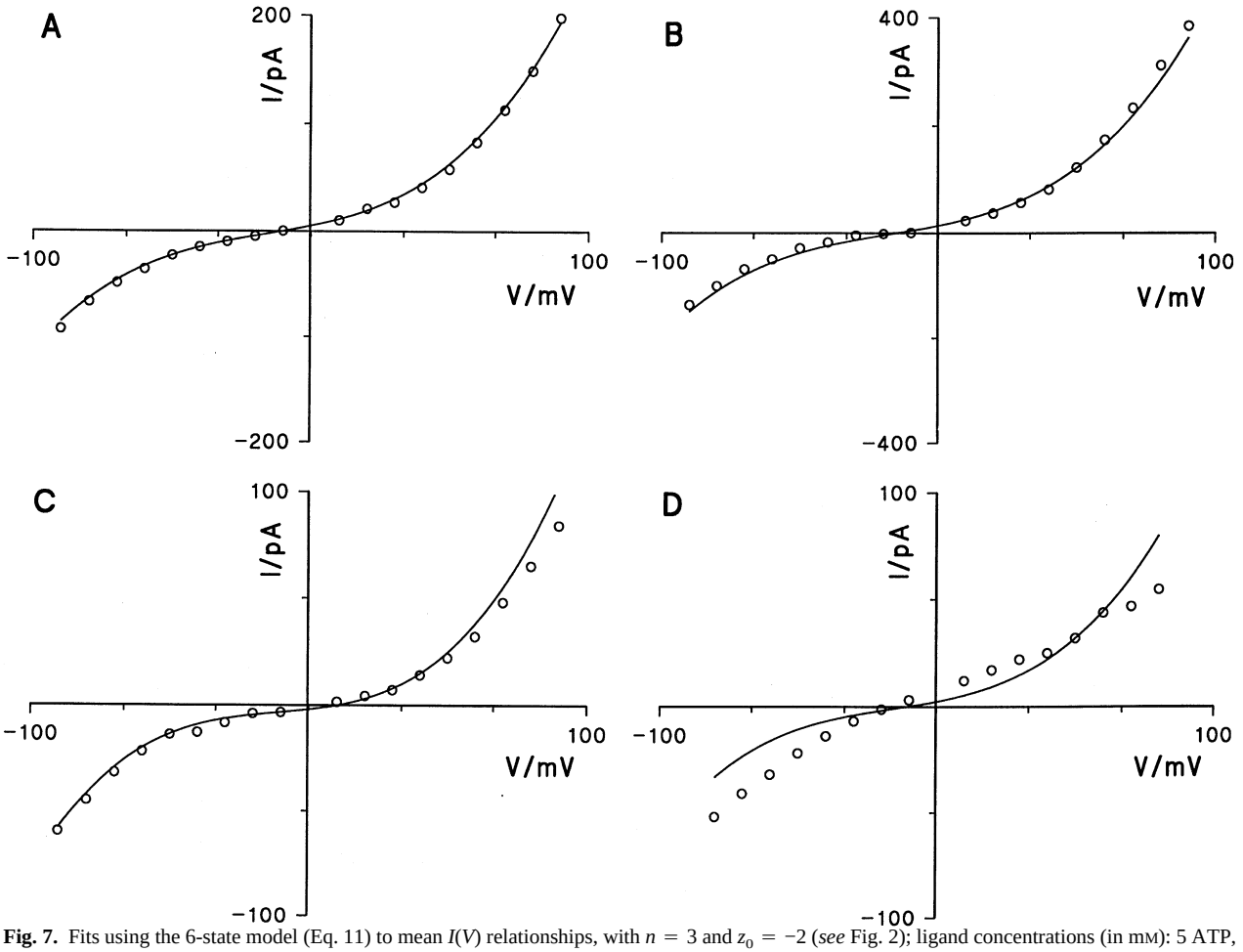

Fig. 7. Fits using the 6-state model (Eq. 11) to mean $I(V)$ relationships, with $n = 3$ and $z_0 = -2$ (*see* Fig. 2); ligand concentrations (in mM): 5 ATP, 5 ADP, 10 P_i except *C* (1 mM ATP). Vacuolar pH 4.3 throughout; pH_{cyt} *A* 7.5, *B* 7.0, *C* and *D* 8.0. Model parameters listed in Table 3.

was not pursued. Table 3 shows a complete set of parameters of the 6-state model for the successful description of four V-ATPase $I(V)$ relationships obtained under different substrate conditions but at constant pH_{vac} of 4.3 For those $I(V)$ relationships obtained at constant pH_{cyt} but variable pH_{vac}, it was not possible to obtain reasonable simultaneous fits, regardless of the binding domain charge (*data not shown*).

Discussion

The aim of this study has been to analyze the pH-dependence of current-voltage relationships of the vacuolar H^+-ATPase in straightforward terms of mass action effects of H^+ as a transport substrate. Both 2- and 6-state models have been employed.

Application of a 2-State Model

Hansen et al. (1981) have introduced the 2-state model as a simplified formalism to describe $I(V)$ relationships of

Table 2. Summary of relative goodness of fits using the 6-state model incorporating partial coupling, applied to data sets obtained at constant pH_{vac} (4.3; Sets *A*, pH_{cyt} 7.5, *B*, pH_{cyt} 7.0, *C*, pH_{cyt} 8.0 and 1 m*M* ATP, *D*, pH_{cyt} 8.0 and 5 mM ATP)

	$n = 2$			$n = 3$		
Charge state of binding domain						
z_0	0	−1	−2	0	−1	−2
z_1	1	0	−1	1	0	−1
z_2	2	1	0	3	2	1
% Error relative to best fit	171	134	230	229	116	100

A simultaneous fit to all data was made, with charge states (z_i) of the active domain and stoichiometry (n) of H^+ translocated per ATP, assuming complete coupling. Error is expressed as relative to the best fit obtained (i.e., $z_0 = -2$, $z_1 = -1$, $z_2 = 1$ and $n = 3$). Unless otherwise stated, the ligand concentrations used were (in mM): 5 ATP, 5 ADP, 10 P_i.

Table 3. Final parameter values employed in the 6-state model with partial coupling; simultaneous fit from experimental conditions *A, B, C* and *D* (i.e., pH_{vac} constant at 4.3 and pH_{cyt} 7.5, 7.0, 8.0, 8.0 respectively).

Rate constant	Experimental condition	Value	Unit
k_{12}^0		1.0	sec^{-1}
k_{21}^0		6.1×10^{-4}	sec^{-1}
k_{23}		4.3×10^{9}	sec^{-1}
k_{32}^0		2.7×10^{13}	$sec^{-1}M^{-2}$
k_{34}^0		3.2×10^{-3}	sec^{-1}
k_{43}^0		1.1	sec^{-1}
k_{41}^0		5.0×10^{9}	$sec^{-1}M^{-2}$
k_{14}		7.0×10^{8}	sec^{-1}
k_{45}		1.4×10^{10}	sec^{-1}
k_{56}^0		3.2×10^{3}	sec^{-1}
k_{65}^0		2.9×10^{3}	sec^{-1}
k_{63}^0		1.6×10^{7}	$sec^{-1}M^{-1}$
k_{36}		1.1×10^{1}	sec^{-1}
k_{54}^0	A	1.0×10^{21}	$sec^{-1}M^{-1}$
	B	2.0×10^{21}	$sec^{-1}M^{-1}$
	C	5.5×10^{21}	$sec^{-1}M^{-1}$
	D	1.1×10^{21}	$sec^{-1}M^{-1}$

The ligand concentrations were (in mM): 5 ATP, 5 ADP, 10 P_i, except for *C* where ATP was 1 mM. Resultant fits to data are shown in Fig. 7.

electrogenic pumps. This model also applies to many other ion transporters. One benefit of this model is its flexibility to describe various shapes of $I(V)$ curves by unique sets of corresponding parameters. For example, $k_{io}k_{oi} \gg \kappa_{io}\kappa_{oi}$ yields sigmoid, supralinear $I(V)$ relationships, whereas $k_{io}k_{oi} \ll \kappa_{io}\kappa_{oi}$ results in superlinear curves with exponentially rising slopes which approach saturation at voltage displacements outside the present experimental range (*see* Hansen et al., 1981). Since both supra- and superlinear curves are represented in this study (e.g., Fig. 6 *F* and *H* and 6 *A–E* and *G* respectively), Eq. 5 has been used successfully to describe those results. It should be noted that, for the purpose of this quasi-empirical fitting, the sign of *z* in Eq. 5 does not matter. Various values of α in Eq. 3 have been tested for description of the $I(V)$ relationships by Eq. 5. In general, small stoichiometric factors generate linearity and large ones more curvature, although a low ratio $k_{io}k_{oi}/(\kappa_{io}\kappa_{oi})$ can also straighten the $I(V)$ curves to some extent. In cases where fitting was performed with α constrained to an integer value, best fits were obtained with $\alpha = 2$; where α was not constrained, its fitted value also converged near 2. For $\alpha = 1$, the resultant curves were too shallow and with $\alpha = 3$ the curvature was too pronounced in all but one case. Figure 6 suggests that the 2-state model is adequate for the data; this holds not only for supralinear curves but also sublinear ones.

However, this 2-state model fails to obey the principle of microscopic reversibility; i.e., the equilibrium voltage (Eq. 7) should have a fixed relationship to the thermodynamic forces of the concentration gradient (here ΔpH) and of the metabolic driving force of the free energy of ATP hydrolysis. Formally, Eq. 7 can be expressed as

$$n = \Delta G_{ATP}/\{F[(59\text{ mV})\Delta\text{pH} - V_r]\}. \quad (13)$$

This relationship has been used by Davies et al. (1994) to estimate transport coupling ratios which apparently varied with imposed values of pH_{cyt} and pH_{vac}. Measured V_r values were not greatly displaced from zero. This means in terms of Eq. 13 that the relatively small ΔpH values used in the experiments yield large values of *n* in the evaluations. Note that Eq. 7 predicts a change in V_r by fully 59 mV per ΔpH, irrespective of the actual value of *n.* Particularly large coupling ratios, *c*, of up to 10 have been reported for F-ATPases (van Walraven et al., 1986) which may also reflect incomplete coupling rather than large stoichiometries. The latter can only be proven if *c* for H^+-driven ATP synthesis/hydrolysis were demonstrated to equal *c* emanating from ATP-driven H^+ translocation.

Application of a 6-State Model with Partial Coupling

With the shortcomings described above, it appears that the 2-state model is not sufficient to describe the experimental data in thermodynamically correct terms but has to be extended by another voltage-sensitive reaction loop. The 6-state reaction scheme in Fig. 2 represents such an extended model. Although some properties of such models have already been discussed in detail by Gradmann et al. (1987) and Klieber and Gradmann (1993), simplifications (such as those described for Class I models by Hansen et al., 1981) are not yet available for description of models with three or more transmembrane steps. Therefore, the explicit 6-state reaction scheme is used here, with the drawback that the numerical solutions cannot be considered unique.

This model is now thermodynamically correct with respect to microscopic reversibility (Eqs. 8) and with respect to integer stoichiometries within the model. Introduction of three transmembrane reactions, where at least two are charge-carrying, circumvents the restrictions of the Class I models. In particular, apparent insensitivity of V_r with respect to substrate gradient (here, ΔpH) can easily be accounted for by mass action; i.e., without changing, or noninteger stoichiometries.

Although the observed thermodynamic properties

could, in principle, be described by a maximum coupling ratio of 2 H^+ translocated per ATP hydrolyzed (one H^+ binding site for each of the two reaction loops), the kinetic properties as expressed by the curvatures of the observed $I(V)$ relationships and numerically reflected in the relative errors of the various fits (Table 2), seem to favor a ratio, n, of at least 3 H^+ per ATP. It should be noted that the best fits were usually obtained with a maximum amount of charge of 2, not 3, for the possible state of charge of the active domain. This finally corresponds to the results of the fits with $\alpha \approx 2$ in the 2-state model (Table 1).

The fact that the 6-state model is able to describe the $I(V)$ curves from all four experimental conditions when pH_{vac} was constant at 4.3 by one common set of reaction kinetic parameters, suggests that the incomplete coupling model may be a realistic one. Even when all eight data sets were subjected to the fitting routine, the program did not converge towards a compromise solution in which all data sets were described with about the same (unsatisfactory) quality, but rather towards good descriptions for $pH_{vac} = 4.3$ and poor ones for all other data sets. These results point to the limits of the model in its present state. It is feasible that further expansion of the model to incorporate sequential and discrete binding of individual H^+ (with differential and pH_{cyt}-dependent pK_a values for each step), rather than a lumped binding reaction of two H^+ at state 4, would allow a greater range of experimental conditions to be modeled successfully. Another possibility is that the pump itself is tightly coupled but can, under unfavorable circumstances, induce a H^+ leak in its immediate environment. Transporters that may act as a leak or a pump have, in fact, been suggested to exist in the plasma membrane of *Chara* (Fisahn, Hansen & Lucas, 1992). This possibility has not been examined here because its formal treatment would require further extension of the model by at least two states.

In summary, apparently high coupling ratios (c) between H^+ translocated and ATP hydrolyzed or synthesised do not necessarily indicate a correspondingly high stoichiometry. Such high values of c may simply reflect incomplete coupling. In this study, the available sets of $I(V)$ data for the vacuolar H^+-ATPase are adequately described in reaction kinetic terms by a model with a coupling of 3 H^+ per ATP. The pump may be assumed to have a domain that is subjected to conformational changes within the process of charge translocation. Whilst it would be premature to relate these findings to the present knowledge of the molecular structure of V-ATPases, the results of the modeling exercise are suggestive of the following: That the domain bears 3 binding sites for H^+, two of which are negatively charged and one electroneutral in their respective unoccupied states, and that reorientation of the 3 binding sites between cytoplasmic and vacuolar sides is possible in various states of occupancy.

Concluding Remarks

The present results and analyses demonstrate the feasibility of a model for incomplete coupling to describe pH-dependent changes in coupling ratio of a V-ATPase. Importantly, the changes in coupling ratio can be accounted for simply through mass action effects of protons at their transport binding sites. There is no need to invoke more complex allosteric effects of pH, at least with respect to modulation of coupling ratio by cytosolic pH.

The authors thank Dr. Peter Rich (Glynn Research Institute) for helpful discussion and are grateful to the Deutsche Forschungsgemeinschaft, the Biotechnology and Biological Sciences Research Council (Grant number 87/PO4043) and the Royal Society (University Research Fellowship to JMD) for financial support. Bafilomycin was a gift from Smith, Kline and Beecham.

References

Bowman, E.J., Siebers, A., Altendorf, K.-H. 1988. Bafilomycins: A class of inhibitors of membrane ATPases from microorganisms, animal cells and plant cells. *Proc. Natl. Acad. Sci. USA* **85:**7872–7876

Davies, J.M., Rea, P.A., Sanders, D. 1991. Vacuolar proton-pumping pyrophosphatase in *Beta vulgaris* shows vectorial activation by potassium. *FEBS Lett.* **278:**66–68

Davies, J.M., Poole, R.J., Rea, P.A., Sanders, D. 1991. Potassium transport into plant vacuoles energized directly by a proton-pumping inorganic pyrophosphatase. *Proc. Natl. Acad. Sci. USA* **89:**11701–11705

Davies, J.M., Poole, R.J., Sanders, D. 1993. The computed free energy change of hydrolysis of inorganic pyrophosphate and ATP: Apparent significance for inorganic pyrophosphate-driven reactions of intermediary metabolism. *Biochim. Biophys. Acta* **1141:**29–36

Davies, J.M., Hunt, I., Sanders, D. 1994. Vacuolar H^+-pumping ATPase variable transport coupling ratio controlled by pH. *Proc. Natl. Acad. Sci. USA* **91:**8547–8551

Fisahn, J., Hansen, U.-P., Lucas, W.J. 1992. Reaction kinetic-model of a proposed plasma-membrane 2-cycle H^+-transport system of *Chara corallina*. *Proc. Natl. Acad. Sci. USA* **89:**3261–3265

Gradmann, D., Klieber, H.-G., Hansen, U.-P. 1987. Reaction kinetic parameters for ion transport from steady-state current-voltage curves. *Biophys. J.* **51:**569–585

Hanrahan, J.W., Alles, W.P., Lewis, S.A. 1985. Single anion-selective channels in basolateral membrane of a mammalian tight epithelium. *Proc. Natl. Acad. Sci. USA* **82:**7791–7795

Hansen, U.-P., Gradmann, D., Sanders, D., Slayman, C.L. 1981. Interpretation of current-voltage relationships for ''active'' ion transport systems: I. Steady-state reaction-kinetic analysis of Class-I mechanisms. *J. Membrane Biol.* **63:**165–190

Harvey, W.R. 1992. Physiology of V-ATPases. *J. Exp. Biol.* **172:**1–17

Klieber, H.-G., Gradmann, D. 1993. Enzyme kinetics of the prime K^+ channel in the tonoplast of *Chara:* Selectivity and inhibition. *J. Membrane Biol.* **132:**253–265

Läuger, P. 1991. Electrogenic Ion Pumps. p. 49. Sinauer, Sunderland, MA.

Läuger, P., Stark, G. 1970. Kinetics of carrier-mediated ion transport across lipid bilayer membranes. *Biochim. Biophys. Acta* **211:**458–466

Rakowski, R.F., Vasilets, L.A., LaTona, J., Schwarz, W. 1991. A negative slope conductance in the current-voltage relationships of the Na^+/K^+ pump in *Xenopus* oocytes produced by reduction of external $[K^+]$. *J. Membrane Biol.* **121:**177–187

Sze, H., Ward, J.M., Lai, S., Perera, I. 1992. Vacuolar-type H^+-translocating ATPases in plant endomembranes: Subunit organization and multigene families. *J. Exp. Biol.* **172:**123–135

van Walvraven, H.S., Haak, N.P., Krab, K., Kraayenhof, R. 1986. *FEBS Lett.* **208:**138–142. Evidence for a high proton translocation stoichiometry of the H^+-ATPase complex in well coupled proteoliposomes reconstituted from a thermophilic cyanobacterium. *FEBS Lett.* **208:**138–142

White, P.J. 1994. Bafilomycin A_1 is a noncompetitive inhibitor of the tonoplast H^+-ATPase of maize coleoptiles. *J. Exp. Bot.* **45:**1397–1402